Agnieszka Żuryń[ORCID], Adrian Krajewski[ORCID]

Department of Histology and Embryology, Faculty of Medicine, Nicolaus Copernicus University in Torun,
Collegium Medicum in Bydgoszcz, Poland

Icaritin induces apoptosis and downregulates RhoA/ROCK pathway in the A549 adenocarcinoma cell line

Corresponding author:

Agnieszka Żuryń, Department of Histol-ogy and Embryology, Faculty of Medicine, Nicolaus Copernicus University in Torun, Collegium Medicum in Bydgoszcz, Poland, e-mail: azuryn@cm.umk.pl

ABSTRACT

Introduction: Icaritin is a prenylflavonoid derivative from a traditional Chinese herb, Epimedium Genus. Icaritin exerts its anti-tumour effects in various cancers mainly by inhibiting cell proliferation, inducing cell differentiation and apoptosis, and suppressing cell migration and invasion. The study aimed to evaluate the effect of icaritin on apoptosis, cell cycle, and expression of selected cell cycle proteins: RhoA, ROCK1, and ROCK2 in the A549 cell line.

Methods: Apoptosis and the cell cycle distribution were evaluated by flow cytometry. Protein expression was measured by conducting a western blot assay and immunofluorescence staining.

Results and conclusions: The study revealed that icaritin induces apoptosis and cell cycle arrest in the G2/M phase in A549 cells. The authors showed that icaritin activates the p53 protein and downregulates Rho/ROCK pathway. Additionally, the decrease in expression of thrombospondin-1 was observed which can be part of the cytoprotective response of A549 cells on ICT treatment.

Key words: RhoA, ROCK1, ROCK2, lung cancer, icaritin (ICT), cell death, thrombospondin-1

Med Res J 2022; 7 (3): 242–248

Introduction

Icaritin is a prenylflavonoid derivative from a tradition-al Chinese herb, Epimedium Genus. Recently, accumu-lating studies have demonstrated an anti-tumour effect of icaritin in various cancer, including solid tumours and haematological cancers, such as lung cancer, hepato-cellular carcinoma, breast cancer, oesophageal cancer, glioblastoma, leukaemia, and lymphoma [1–7].

Rho/Rho-associated protein kinases (ROCK) path-way plays a critical role in the regulation of cancer motility and invasion. Control of cell motility in the actin cytoskeleton creates the potential for regulating tumour cell metastasis [8]. The Rho family of GTPases is a family of small monomeric G proteins that belong to the Ras superfamily of GTPases and comprises more than 50 members that share several common features: their molecular weight (18–28 kDa), their C-terminal polyisoprenylation region, and the property to bind to and hydrolase guanine nucleotides [9]. Rho GTPases bind to a wide range of effector proteins and play central roles in the regulation of the actin and microtubule cy-toskeletons and gene transcription [10]. Through these effects, Rho family proteins influence many normal cellular functions such as adhesion, polarity, motility, and invasion, as well as cycle progression and surviv-al [11, 12]. Deregulation of Rho GTPases is linked to many of the hallmarks of cancer, including oncogenic transformation, cell survival, and tumour metabolism as well as metastasis. While some consequences of deregulated Rho family signalling can be considered pro-tumourigenic, several cellular processes stimulated by Rho family proteins – such as the role of Rac1 in apoptosis and maintenance of apicobasal polarity can be considered to antagonize tumour formation and pro-gression [13]. The anti-tumourigenic effects of the Rho family protein must be sufficiently differentiated from those pro-oncogenic functions to avoid undermining the therapeutic benefits to be achieved by pharmaco-logically antagonizing Rho GTPases [14].

The present study investigates the antitumour properties of icaritin and conducts molecular analysis to show that ICT exerts its effect *via* the RhoA/ROCK pathway.

Material and methods

Cell culture and icaritin treatment

The human non-small cell lung carcinoma cell line A549 was purchased from the American Type Culture Collection (USA). The cells were cultured in monolayers at 37ºC in a humidified CO_2 incubator (5% CO_2) in DMEM (Gibco, USA) supplemented with 10% foetal bovine serum (FBS; Gibco, USA) and 50 μg/ml of gentamycin (Sigma-Aldrich, Germany). Twenty-four hours after seeding, the cells were treated with icaritin (Sigma-Aldrich, Germany) for 24 and 48 h, and the following experimental procedures were performed [15].

MTT assay

Twenty-four hours before icaritin treatment, the A549 cells were seeded in 12-well plates. Then cells were treated with appropriate icaritin concentrations for 24 and 48 hours. Following the treatment, cells were washed with PBS and 1ml of DMEM without phenol red and 100μl of the thiazolyl blue tetrazolium bromide (MTT) working solution Sigma-Aldrich; 5 mg/mL in PBS) were added to each well and incubated for 3 hours. Formazan crystals were diluted in isopropanol and the absorbance was read at 570 nm in a spectrophotometer (Spectra Academy, K-MAC, Daejeon, Korea) [15].

Annexin V/propidium iodide (PI) binding assay

To assess the mode of cell death, the Alexa Fluor 488 Annexin V/Dead Cell Apoptosis Kit (Invitrogen, USA) was used according to the manufacturer's instructions. In short, after the ICT treatment, the cells were collected from 6-well plates using the trypsin-EDTA solution, centrifuged at 300 × g for 8 min, resuspended in ABB (annexin binding buffer), and incubated with Annexin V Alexa Fluor® 488 and propidium iodide at room temperature in the dark for 20 minutes. The cells were examined using a Guava 6HT-2L Cytometer (Merck). The data were analysed by InCyte software (version 4.3; Merck, Germany) and expressed as the percentage of cells in each population (viable Annexin V-/PI-; early apoptotic Annexin V+/PI-; late apoptotic Annexin V+/PI+; necrotic Annexin V-/PI+) [15].

DNA content analysis

For DNA content analysis, the Guava Cell Cycle Reagent (Merck, Germany) was used according to the manufacturer's instructions. Briefly, the cells were

harvested from 6-well plates by trypsinization, rinsed with PBS, fixed in ice-cold 70% ethanol at 4°C, and left at -20°C overnight. The cells were then centrifuged at 650 × g for 5 min and washed with PBS. After centrifugation at 500 × g for 7 min, the cells were resuspended in Guava Cell Cycle Reagent. Following a 30-min incubation at RT in the dark, the cells were analysed using Guava 6HT-2L Cytometer (Merck, Germany), and the percentage of cells in each phase of the cell cycle was determined using InCyte software (version 3.3; Merck, Germany) [15].

Immunofluorescence staining

A549 cells growing on coverslips were fixed in 4% paraformaldehyde (15 min, RT) and then washed with PBS (3 x 5 min). After that, the cells were incubated in a permeabilization solution (0.1% Triton X-100 in PBS) and blocked with 3% BSA. After permeabilization, the cells were incubated with the appropriate primary antibody, washed three times with PBS, and incubated with Alexa Fluor 488 goat anti-mouse IgG (Invitrogen, Molecular Probes, USA) or with Alexa Fluor 488 goat anti-rabbit IgG (Invitrogen, Molecular Probes, USA) (60 min, in the dark). Nuclear staining was performed with DAPI (Sigma-Aldrich, Germany). Contract labelling with Alexa Fluor 594 phalloidin (ThermoFisher Scientific, USA) was used additionally. After incubation, the cells were washed with PBS and then mounted on microscope slides in Aqua Poly/Mount (Polysciences, Inc, USA). The cells were examined using a C1 laser-scanning confocal microscopy system (Nikon, Tokyo, Japan) with a 100x oil immersion objective. Fluorescence images were obtained and analysed with Nikon EZ-C1 software (Ver3.80; Nikon Instruments, USA) [15].

Western Blot assay

For semi-quantitative protein expression measurement, Western Blot analysis was conducted. Whole-cell lysates were obtained from lysis in RIPA buffer (Merck, Germany). Following normalization of the protein concentration using the BCA protein assay kit (Thermo Scientific Pierce, USA), equal amounts of protein (25 μg of total protein per lane) were separated using 4–12% or 16% NuPAGE Bis-Tris Gel (Novex/Life Technologies, Carlsbad, CA, USA) and transferred onto nitrocellulose membranes using the iBlot dry western blotting system (Invitrogen/Life Technologies, USA). The membrane was processed in the iBind Flex Western Blot system following the manufacturer's protocol. Bands were detected using a 1-Step™ Ultra TMB-Blotting solution [15].

Antibody list

Rho A (ThermoFisher, 1B8-1C7, USA), ROCK1 (Abcam, ab58305, GB), ROCK2 (Abcam, ab71598, GB),

p53 (ThermoFisher, Pab 240, USA), thrombospondin-1 (ThermoFisher, MA5-13398, USA), GAPDH (ThermoFisher, MA5-15738, USA), Phalloidin-AF488 (ThermoFisher, A12379, USA)

Statistical analysis

The analysis was performed using statistical software (GraphPad Prism 9, USA). The data were compared with the nonparametric Mann–Whitney U test or nonparametric Kruskal-Wallis test with Dunn's multiple comparisons test, and the changes were considered statistically significant at the level of $p < 0.05$.

Results and discussion

Icaritin induces apoptosis and cell cycle arrest in A549 non-small cell lung cancer cell line

The present study shows that icaritin has the potential to inhibit lung cancer progression, limiting proliferation through cell cycle arrest and inducing apoptosis. The treatment of the A549 cell line with icaritin resulted in a significant decrease in viability measured with MTT assay (Fig. 1). Annexin V/PI staining showed that icaritin induces significant apoptosis after 24h and 48h treatment (Fig. 2). These results are in line with other studies that icaritin could be an effective drug in lung cancer therapy. Zheng et al. showed that icaritin can induce apoptosis and S-phase cell cycle arrest *via the* MAPK pathway [6]. Additionally, it has been presented that icaritin can limit lung cancer-induced osteoclastogenesis. The authors suggested that icaritin has the potential to reduce lung-cancer-induced bone destruction through the modulation of the AMPK/mTOR pathway [16]. Interestingly, the silencing of AMPKα1 sensitizes colon cancer cells to ICT-induced apoptosis [17]. It is possible, that the effect of ICT on A549 cells could be enhanced when AMPK inhibitors or autophagy inhibitors will be used as a co-treatment. *In vivo* studies revealed that ICT can enhance CD8+ T cell infiltration. The chemokines produced by T-cells, can modify the tumour microenvironment and improve the patient outcome [18]. Several studies showed that icaritin can limit the proliferation rate inducing cell cycle arrest. Zheng et al. showed that icaritin induces S phase arrest in A549 [6]. However, in the present study, similar doses were used, and an increase in the G2/M population (Fig. 3) and the activation of p53 protein (Fig. 4 and Fig. 5 B) were observed. The differences can result from seeding densities and different times from seeding to treatment. Other studies show that icaritin induces cell cycle arrest in both S and G2/M phases. In extranodal NK/T-cell lymphoma (ENKL) cell lines ICT induced cell cycle arrest in the G2/M phase

and apoptosis *via* inhibition of Stat3 and Akt pathways through LMP1 downregulation. The effectiveness of icaritin was higher when cells were additionally treated with ganciclovir [5]. By inducing ROS generation and subsequently DNA double-strand breaks icaritin arrests cervical cancer cells in the G2/M phase [19]. This data and other studies show that icaritin can be an effective drug in treating solid tumours and haematological malignancies. Already the phase III study of icaritin versus sorafenib in PD-L1 positive advanced hepatocellular carcinoma (NCT03236649) is ongoing and that shows that ICT has real potential to be an effective drug.

### Icaritin downregulates RhoA, ROCK1 and ROCK2 expression

To assess the effect of icaritin on actin reorganization, the cells treated with ICT were stained with phalloidin-Alexa 488 conjugate. As presented in Figure 5A the F-actin cytoskeleton is severely disrupted after the
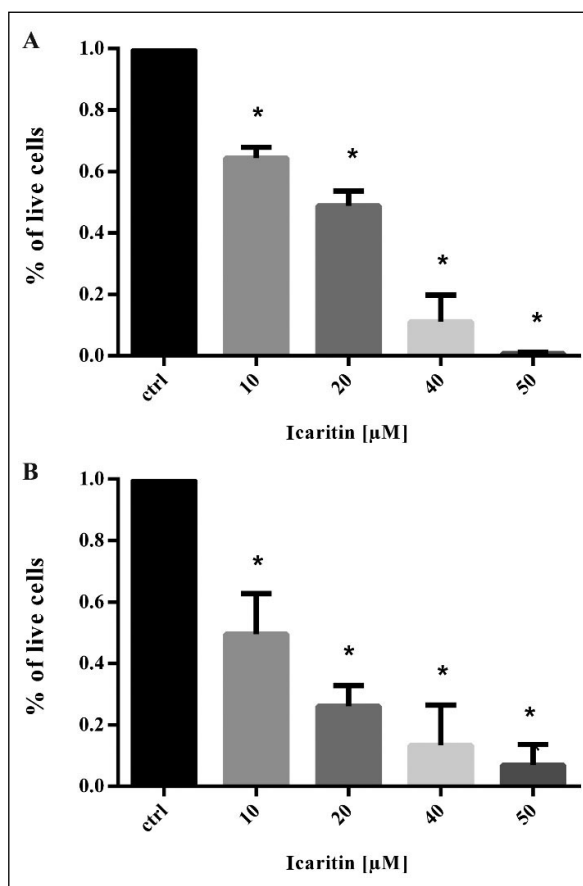

Figure 1. The MTT assays show a decrease in cellular viability after the icaritin treatment. **A.** The A549 cell line treated with ICT for 24h. **B.** The A549 cell line treated with ICT for 24h. Asterisks indicate statistically significant results ($p < 0.05$)
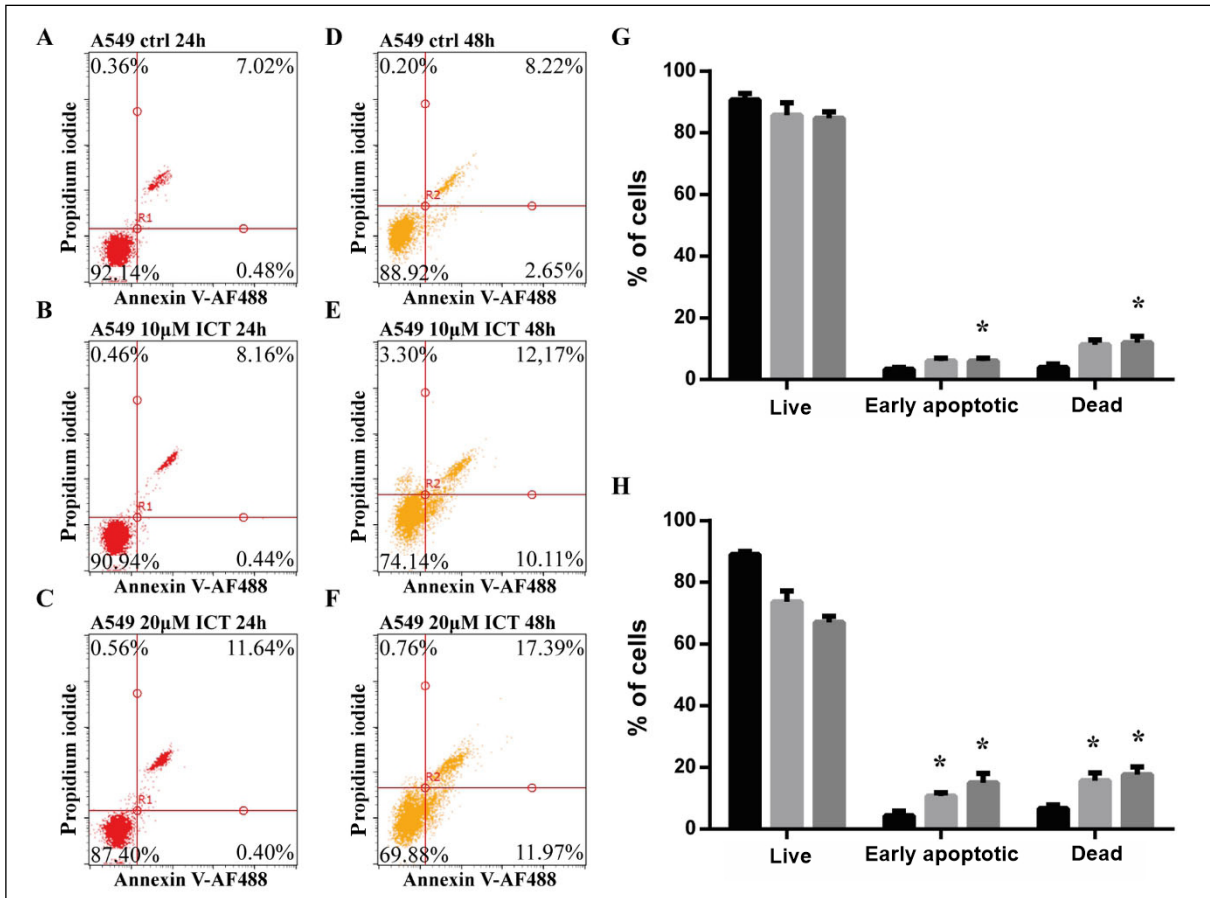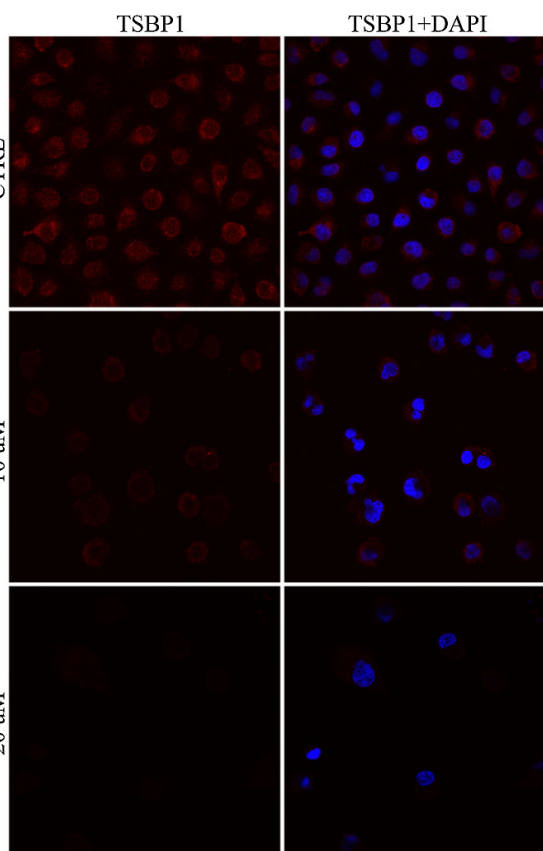
**Figure 2.** The icaritin induces apoptosis in A549 cells
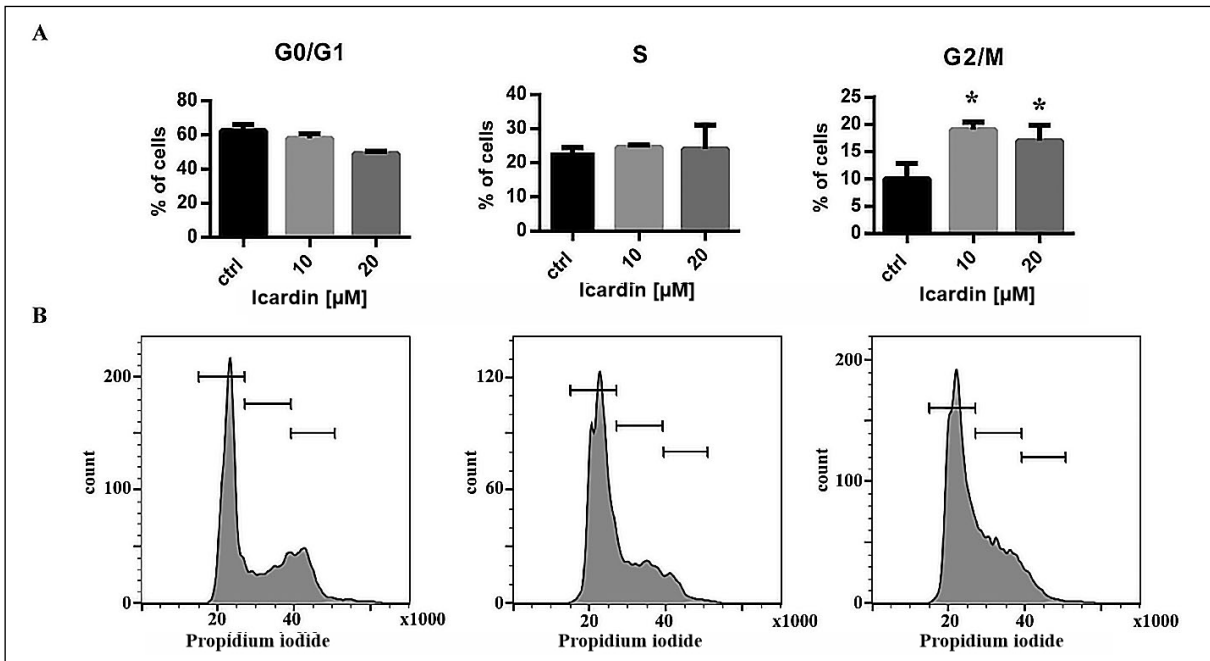
Figure 3. Icaritin induces cell cycle arrest. After the ICT treatment, a significant increase in the percentage of G2/M phase cells was observed
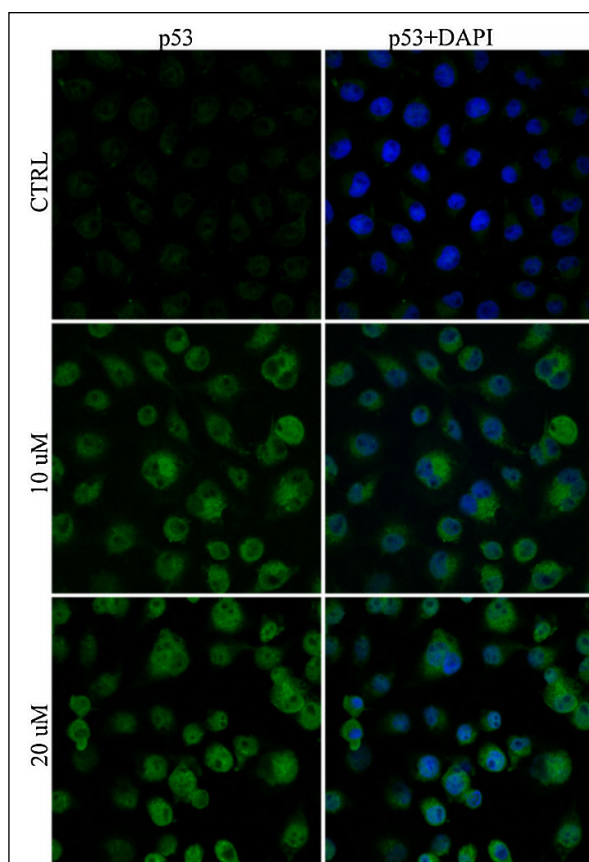
Figure 4. The immunofluorescence image of p53 activation after the ICT treatment

Figure 6. The expression of thrombospondin-1 is significantly downregulated after the ICT treatment
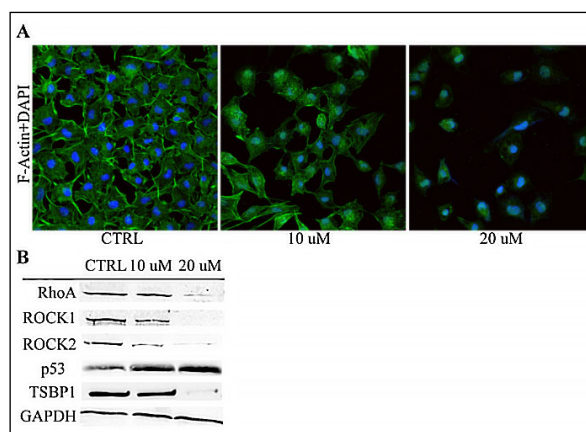
Figure 5. A. The effect of ICT on the F-actin cytoskeleton reorganization. The disruption of stress fibres after the treatment with 20μM ICT is visible. **B.** The western blots revealed a significant downregulation of the RhoA/ROCK pathway, p53 activation, and loss of thrombospondin-1 expression in the A549 cell line

icaritin treatment compared with the control with integrated and organized filamentous actin. To further investigate the mechanism underlying the F-actin reorganization,

a western blot assay was conducted to investigate if the observed phenomenon is associated with the inhibition of the ROCK pathway. The results showed that Rho A, ROCK1, and ROCK2 are significantly downregulated after the icaritin treatment. The ROCK pathway is commonly upregulated in NSCLC and is associated with a more aggressive phenotype. Hu et al. showed that ROCK1 overexpression confers to worse survival and regulates migration and invasion of NSCLC cells. ROCK1 supports cancer progression through the activation of PTEN, phosphorylation of PI3K/AKT, and then FAK phosphorylation [20]. It has been shown that ROCK inhibitors can be effective in inhibiting the proliferation and invasion of lung cancer cell lines. Selective inhibition of the ROCK1/2 kinases results in reduced anchorage-independent growth and invasion of different lung cancer cell lines [21]. Another study showed that A549 cells incubated with baicalein were characterized by retarded ability to form vasculogenic mimicry and reduced tumourigenicity. These observations coincided with downregulated RhoA/ROCK proteins and impaired F-actin cytoskeleton [22]. These results agree with the authors' observations involving ICT treatment and confirm that inhibiting the ROCK pathway is a viable option for targeting lung cancer. These two drugs may share a similar mechanism of action.

Downregulation of thrombospondin-1 after icaritin treatment

During the screening for the potential targets affected by icaritin, it was found that the treatment A549 cell with ICT significantly decreases the expression of thrombospondin-1 (Fig. 5B). The same phenomenon has been observed under the fluorescence microscope (Fig. 6). Thrombospondin-1 is a glycoprotein involved in forming the cancer microenvironment. Thrombospondin-1 is best known for its anti-angiogenic activity, however, the number of pathways that thrombospondin-1 affects is still growing. The role of thrombospondin-1 in adenocarcinoma is relatively poorly understood. Chen et al. showed that the expression of TSP1 in non-small cell lung cancer tissues is significantly lower and correlates with higher microvessel densities, especially in higher-grade and metastatic NSCLC [23]. Additionally, high serum levels of TSP1 were associated with a better prognosis for the patients [24]. On the other hand, some tumours seem to be driven by the thrombospondin-1 expression. Increased levels of thrombospondin-1 were found in higher-grade gliomas. It was reported that thrombospondin-1 is regulated by TGF 1 via SMAD3 promoter binding. The silencing of TSBP1 resulted in reduced invasion and decreased the number of small vessels [25]. Thrombospondin-1 is involved in the regulation of chemotherapy-induced senescence. A low level of TSBP1 was a predictor of unsuccessful therapy in patients with TNBC breast cancer. TSBP1 inhibited senescence escape in breast cancer cells and reduced proliferation binding the CD47 protein [26]. Treating the primary human trabecular meshwork cells (hTM) with selective ROCK inhibitor Y39983, resulted in the downregulation of TSBP1. Moreover, silencing TSBP1 in hTM cells decreases migration and invasion. It has been proposed that TSBP1 mediates the inhibition of ROCK and it can be hypothesized that a similar novel mechanism is involved in icaritin influence on the A549 cell line, however, this has to be confirmed in the future [27]. Cutaneous melanoma cell lines are characterized by strong TSBP-1 expression, which correlates with the set of genes involved in melanoma motility and metastasis. TSBP-1 expression was positively associated with the production of FGF-2 and VEGF/VEGFR-1. Moreover, the expression of these genes was negatively correlated with Slug — the protein crucial for the motility potential. The TSBP-1 downregulation can be the alternative pathway that drives tumour metastasis and its inhibition could be a potential therapeutic target [28]. It is also possible that the decrease in thrombospondin-1 levels is part of the protective response and limits the efficiency of icaritin in the A549 cell line. An additional study involving the re-introducing of the TSBP-1 into the treated cells is needed to determine the role of this protein in lung cancer during the drug treatment.

Conclusions

In conclusion, the present study demonstrated that icaritin effectively induces apoptosis and cell cycle arrest in the A549 lung adenocarcinoma cell line. Molecular studies revealed the downregulation of the RhoA/ROCK pathway after the icaritin treatment. The potential role of thrombospondin-1 in the response to the icaritin administration has been proposed, however, the details and nature of TSBP1 downregulation must be elucidated in the future.

Conflict of interests: *None.*

References

1. Guo Y, Zhang X, Meng J. and Wang Z-Y: An anticancer agent icaritin induces sustained activation of the extracellular signal-regulated kinase (ERK) pathway and inhibits growth of breast cancer cells. Eur J Pharmacol 658: 114–122. ; 2011.
2. Han S, Gou Y, Jin D, et al. and Dong X: Effects of Icaritin on the physiological activities of esophageal cancer stem cells. Biochem Biophys Res Commun 504: 792–796. ; 2018.
3. Liu Y, Shi L, Liu Y, et al. Activation of PPAR mediates icaritin-induced cell cycle arrest and apoptosis in glioblastoma multiforme. Biomed Pharmacother. 2018; 100: 358–366, doi: 10.1016/j.biopha.2018.02.006, indexed in Pubmed: 29453045.
4. Sun Li, Peng Q, Qu L, et al. Anticancer agent icaritin induces apoptosis through caspase-dependent pathways in human hepatocellular carcinoma cells. Mol Med Rep. 2015; 11(4): 3094–3100, doi: 10.3892/mmr.2014.3007, indexed in Pubmed: 25434584.
5. Wu T, Wang S, Wu J, et al. Icaritin induces lytic cytotoxicity in extranodal NK/T-cell lymphoma. J Exp Clin Cancer Res. 2015; 34: 17, doi: 10.1186/s13046-015-0133-x, indexed in Pubmed: 25887673.
6. Zheng Q, Liu WW, Li B, et al. Anticancer effect of icaritin on human lung cancer cells through inducing S phase cell cycle arrest and apoptosis. J Huazhong Univ Sci Technolog Med Sci. 2014; 34(4): 497–503, doi: 10.1007/s11596-014-1305-1, indexed in Pubmed: 25135717.
7. Zhu S, Wang Z, Li Z, et al. Icaritin suppresses multiple myeloma, by inhibiting IL-6/JAK2/STAT3. Oncotarget. 2015; 6(12): 10460–10472, doi: 10.18632/oncotarget.3399, indexed in Pubmed: 25865044.
8. Matsuoka T, Yashiro M. Rho/ROCK signaling in motility and metastasis of gastric cancer. World J Gastroenterol. 2014; 20(38): 13756–13766, doi: 10.3748/wjg.v20.i38.13756, indexed in Pubmed: 25320513.
9. Marei H, Malliri A. Rac1 in human diseases: The therapeutic potential of targeting Rac1 signaling regulatory mechanisms. Small GTPases. 2017; 8(3): 139–163, doi: 10.1080/21541248.2016.1211398, indexed in Pubmed: 27442895.
10. Hall A. Rho family GTPases. Biochem Soc Trans 40: 1378. 1382; 2012.
11. Orgaz JL, Herraiz C, Sanz-Moreno V. Rho GTPases modulate malignant transformation of tumor cells. Small GTPases. 2014; 5: e29019, doi: 10.4161/sgtp.29019, indexed in Pubmed: 25036871.
12. Sadok A, Marshall CJ. Rho GTPases: masters of cell migration. Small GTPases. 2014; 5: e29710, doi: 10.4161/sgtp.29710, indexed in Pubmed: 24978113.

13. Mack NA, Whalley HJ, Castillo-Lluva S, et al. The diverse roles of Rac signaling in tumorigenesis. Cell Cycle. 2011; 10(10): 1571–1581, doi: 10.4161/cc.10.10.15612, indexed in Pubmed: 21478669.

14. Porter AP, Papaioannou A, Malliri A. Deregulation of Rho GT-Pases in cancer. Small GTPases. 2016; 7(3): 123–138, doi: 10.1080/21541248.2016.1173767, indexed in Pubmed: 27104658.

15. Żuryń A, Krajewski A. KlimaszewskaWiśniewska A, Grzanka A and Grzanka D: Expression of cyclin B1, D1 and K in nonsmall cell lung cancer H1299 cells following treatment with sulforaphane. Oncol Rep. ; 2018.

16. Zhao X, Lin Y, Jiang B, et al. and Zeng J: Icaritin inhibits lung cancer-induced osteoclastogenesis by suppressing the expression of IL-6 and TNF-a and through AMPK/mTOR signaling pathway. Anticancer Drugs 31: 1004. 1011; 2020.

17. Zhou C, Gu J, Zhang G, et al. Chen M-B and Xu D: AMPK-autophagy inhibition sensitizes icaritin-induced anti-colorectal cancer cell activity. Oncotarget 8: 14736–1. 4747; 2017.

18. Huang C, Li Z, Zhu J, et al. Systems pharmacology dissection of targeting tumor microenvironment to enhance cytotoxic T lymphocyte responses in lung cancer. Aging (Albany NY). 2021; 13(2): 2912–2940, doi: 10.18632/aging.202410, indexed in Pubmed: 33460401.

19. Chen X, Song L, Hou Y. and Li F: Reactive oxygen species induced by icaritin promote DNA strand breaks and apoptosis in human cervical cancer cells. Oncol Rep. ; 2018.

20. Hu C, Zhou H, Liu Y, et al. ROCK1 promotes migration and invasion of nonsmallcell lung cancer cells through the PTEN/PI3K/FAK pathway. Int J Oncol. 2019; 55(4): 833–844, doi: 10.3892/ijo.2019.4864, indexed in Pubmed: 31485605.

21. Vigil D, Kim TY, Plachco A, et al. ROCK1 and ROCK2 are required for non-small cell lung cancer anchorage-independent growth and inva-

sion. Cancer Res. 2012; 72(20): 5338–5347, doi: 10.1158/0008-5472. CAN-11-2373, indexed in Pubmed: 22942252.

22. Zhang Z, Nong Li, Chen M, et al. Baicalein suppresses vasculogenic mimicry through inhibiting RhoA/ROCK expression in lung cancer A549 cell line. Acta Biochim Biophys Sin (Shanghai). 2020; 52(9): 1007–1015, doi: 10.1093/abbs/gmaa075, indexed in Pubmed: 32672788.

23. Chen Z, Le H, Zhang Y, et al. and Li W: Microvessel Density and Expression of Thrombospondin-1 in Non-small Cell Lung Cancer and Their Correlation with Clinicopathological Features. J Int Med Res 37: 551–556. ; 2009.

24. Rouanne M, Adam J, Goubar A, et al. Osteopontin and thrombos-pondin-1 play opposite roles in promoting tumor aggressiveness of primary resected non-small cell lung cancer. BMC Cancer. 2016; 16: 483, doi: 10.1186/s12885-016-2541-5, indexed in Pubmed: 27422280.

25. Daubon T, Léon C, Clarke K, et al. Deciphering the complex role of throm-bospondin-1 in glioblastoma development. Nat Commun. 2019; 10(1): 1146, doi: 10.1038/s41467-019-08480-y, indexed in Pubmed: 30850588.

26. Guillon J, Petit C, Moreau M, et al. Regulation of senescence escape by TSP1 and CD47 following chemotherapy treatment. Cell Death Dis. 2019; 10(3): 199, doi: 10.1038/s41419-019-1406-7, indexed in Pubmed: 30814491.

27. Shan SW, Do CW, Lam TC, et al. Thrombospondin-1 mediates Rho--kinase inhibitor-induced increase in outflow-facility. J Cell Physiol. 2021; 236(12): 8226–8238, doi: 10.1002/jcp.30492, indexed in Pubmed: 34180057.

28. Borsotti P, Ghilardi C, Ostano P, et al. Thrombospondin-1 is part of a Slug--independent motility and metastatic program in cutaneous melanoma, in association with VEGFR-1 and FGF-2. Pigment Cell Melanoma Res. 2015; 28(1): 73–81, doi: 10.1111/pcmr.12319, indexed in Pubmed: 25256553.